analytical chemistry

pubs.acs.org/ac
Article

Methods for Oxygen Determination in an NMR Bioreactor as a Surrogate Marker for Metabolomic Studies in Living Cell Cultures

Christian Urzì, Christoph Meyer, Jean-Marc Nuoffer,[#] and Peter Vermathen*,[#]

Cite This: https://doi.org/10.1021/acs.analchem.3c02314
Read Online

ABSTRACT: Nuclear magnetic resonance (NMR) approaches have been described as a powerful method for measuring oxygen in tissue cultures and body fluids by using relaxation time dependencies of substances on pO_2. The present NMR study describes methods to longitudinally monitor global, in situ intracellular, and spatially resolved oxygen tension in culture media and 3D cell cultures using relaxation times of water without the need to use external sensors. ^{1}H NMR measurements of water using a modified inversion recovery pulse scheme were employed for global, i.e., intra- and extracellular oxygen estimation in an NMR-bioreactor. The combination of ^{1}H relaxation time T_1 and diffusion measurements of water was employed for in situ cellular oxygen content determination. Spatially selective water relaxation time estimations were used for spatially resolved oxygen quantification along the NMR tube length. The inclusion in a study protocol of the presented techniques for oxygen quantification, as a surrogate marker of oxidative phosphorylation (OXPHOS), provides the possibility to measure mitochondrial respiration and metabolic changes simultaneously.

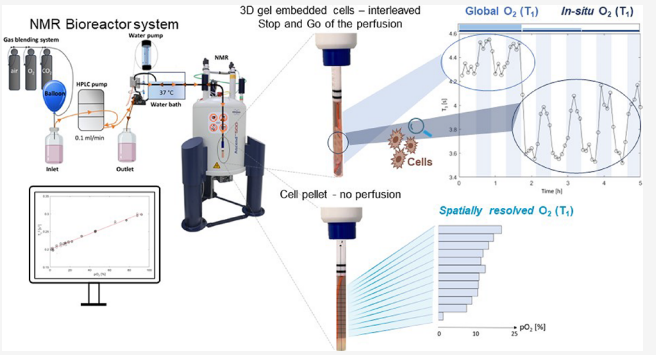

INTRODUCTION

The solubility of oxygen (O_2) is a fundamental parameter in various fields of biosciences such as physiology and biochemistry. Dissolved oxygen is a critical factor that determines different cellular aspects, as it is known to have an impact on both cell viability and function (Graeber,' et al., 1994, Mercille & Massie, 1994).[1,2] It has a regulatory function in many signaling pathways and it is used as a substrate by over a hundred known enzymatic reactions (Erecinska et al., 2001).[3] Oxygen is the primary oxidant in energy-producing reactions; therefore, it plays an essential role in the energy metabolism of all cells.[4] Mitochondrial oxidative phosphorylation (OXPHOS) requires the presence of oxygen, which acts as the final electron acceptor in the electron transport chain. In a series of reactions, respiratory chain complexes pump protons across the inner mitochondrial membrane and transport electrons, resulting in adenosine triphosphate (ATP) production. Shortage of ATP is considered the main reason for most of the heterogeneous and multisystemic mitochondrial disorders. For this reason, determination of oxygenation and oxygen consumption as a surrogate marker of the OXPHOS is highly valuable for the assessment of mitopathogenic mechanisms.[5] In addition, mitochondrial dysfunction is often characterized by a redox state imbalance, which also affects cellular metabolism. Therefore, the simultaneous monitoring of both mitochondrial respiration and metabolome may provide new insight into these biological processes.

Several methods have been described for measuring oxygen in mammalian tissue cultures and body fluids, such as amperometric oxygen sensors,[6] optical sensors,[7,8] respirometry analyzer (such as Seahorse XF Analyzer (Agilent, US) or Oroboros O2k-FluoroRespirometer (Oroboros Instruments, Austria)[9−12]), and nuclear magnetic resonance (NMR) approaches using relaxation time dependencies of substances on oxygen tension (pO_2). However, only NMR approaches provide comprehensive metabolomic information along with oxygen assessment and are thereby uniquely capable of monitoring the interplay between mitochondrial respiration and cellular metabolism.

Numerous previous *in vivo*[13] and *ex vivo*[14,15] studies have used ^{19}F NMR of supplemented perfluorocarbons (PFCs) to determine the oxygen content via relaxation time measurements. Similarly, we have previously shown the feasibility of measuring oxygenation of living fibroblasts embedded in a collagen-based 3D matrix by ^{19}F NMR measurements of T_1 spin−lattice relaxation times of supplemented perfluorotributylamine (PFTBA)-doped microcarrier beads.[5] Similar to what

Received: May 29, 2023
Revised: October 20, 2023
Accepted: October 20, 2023

also other groups have shown,[16,17] a perfused NMR bioreactor system was established based on the InsightMR flow unit and real-time metabolic changes of small molecules by ^{1}H NMR and concurrent oxygenation levels were determined during periodically flow-rate interruption experiments ("stop and go"), and upon applying a substrate inhibition protocol during constant perfusion. However, a deterioration of NMR signal quality caused by these microcarrier beads was observed,[18] likely due to susceptibility differences, and a frequent insensitivity to oxygen changes was encountered, probably due to Ostwald ripening leading to the formation of large PFTBA droplets.[4,19] Owing to their both highly hydrophobic and lipophobic nature,[20] PFCs require the formation of aqueous emulsions for biological studies. However, these emulsions can become unstable and lead to coalescence, resulting in larger droplets and lower PFCs, corresponding to a decreased sensitivity to oxygen changes. Most importantly, proton resonances from emulsions overlap and mask metabolites in the NMR spectra.

Therefore, the capability to measure oxygenation and oxygen consumption by using ^{1}H NMR, without introducing artificial oxygen carriers into the 3D scaffold, would allow for the preservation of the NMR signal quality and simplify the scaffold realization procedure. The influence of paramagnetic oxygen on the proton spin−lattice relaxation time T_1 of water was addressed in earlier studies, in which the solvation of paramagnetic molecular oxygen in protonic solvents was found to decrease the spin−lattice relaxation time by dipole−dipole and hyperfine interactions (Mihrej, 1965).[21] Moreover, the linear dependence of the spin−lattice relaxation rate (i.e., $1/T_1$) of water on the concentration of oxygen was demonstrated (Mihrej, 1965).

A common problem in NMR measurements of very strong signals (e.g., ^{1}H signal of water) is the generation of induced currents in the NMR coil, which generate magnetic fields that broaden the width of the resonance and accelerate longitudinal recovery of the magnetization.[22] This phenomenon, called radiation damping (RD), affects quantitative T_1 estimations via inversion recovery (IR) experiments by deviating the expected exponential recovery curve to an abrupt, broken curve.[23] Therefore, suppression of RD is needed in IR experiments for relaxation determination of water.

In our previous study, the living cells only contributed 1−2% to the overall sample volume within the NMR sensitive region of the bioreactor tube.[18] Similarly, in previous *ex vivo* studies of perfused cells the cell fraction was low compared to the predominating extracellular fraction.[24,25] Therefore, measuring oxygenation and cellular oxygen consumption using ^{1}H T_1 times of overall water within the NMR sensitive region of the bioreactor tube provides primarily extracellular levels and *in situ* intracellular oxygenation determination thus appears unfeasible. We have previously shown the capability to separately measure the intracellular and extracellular water contribution using diffusion NMR. Correspondingly, the combination of proton spin−lattice relaxation time T_1 and diffusion measurements of water would allow for the characterization of T_1 relaxation times of *in situ* (i.e., in the intracellular space and in proximity to the cells, where the exchange between intra- and extracellular water molecules takes place) slow diffusing water contributions.

While the measurement of the global T_1 relaxation time of the water resonance is extremely useful to monitor the global oxygen tension in the perfused cell culture system, a spatially resolved oxygen concentration determination along the 3D scaffold volume would add even more information. Spatially resolved real-time monitoring of oxygen consumption non-invasively using two separated layers of PFC-doped beads and employing slice selective ^{19}F T_1 relaxation rate measurements was described by Pilatus et al.[14] Upon inhibitor challenges, they showed corresponding changes in cellular oxygen consumption. Spatial localization techniques by employing either radio frequency (RF), static, or time-dependent magnetic field gradients have been described to restrict data acquisition to single or multiple selected volumes.[14,15,26] Magnetic field gradients during signal acquisition might be used in combination with T_1 relaxation time estimations to determine the localized oxygen tension. Using this approach, spatial oxygen gradients and comprehensive interplay between fluid dynamics and oxygen transport phenomena may be studied.

To our knowledge, no study has focused on the determination of global, *in situ* directly at the cells, and spatial oxygenation and oxygen consumption rate using proton spin−lattice relaxation time T_1 of water in living cell cultures inside the NMR. Hence, the aims of this study are

1. Global oxygen content determination in the NMR bioreactor tube using water relaxation time estimations suppressing RD and comparing it with the previously applied estimation via ^{19}F NMR using PFCs;
2. *In situ* intracellular oxygen content determination in the 3D cell culture sample by combining proton relaxation time T_1 and diffusion measurements of water at high diffusion-weighting factors;
3. Spatially resolved oxygen quantification along the NMR bioreactor tube length using spatially selective water relaxation time estimations.

EXPERIMENTAL SECTION

2D Cell Culture. Human fibroblasts, derived from skin biopsy of healthy controls in routine diagnostics, were supplied to the routine cell culture laboratory of the Center of Laboratory Medicine of the University Hospital Bern. The cells were cultivated in 2D as performed previously.[5,18] Briefly, the control fibroblast cell line was cultured in MEM supplemented with 10% fetal calf serum, 1× nonessential amino acids (100 μM glycine, L-alanine, L-asparagine, L-aspartic acid, L-glutamic acid, L-proline, L-serine) (GIBCO/Invitrogen, Carlsbad, CA, USA), 2 mM L-glutamine, 200 μM uridine, 1 mM sodium pyruvate, 100 U mL^{-1} penicillin, and 100 μg mL^{-1} streptomycin and 10 μg mL^{-1} chlortetracycline at 310 K and 5% CO_2 in a cell culture incubator. The medium was exchanged between two and three times a week, and fibroblasts were passaged using 0.05% trypsin−EDTA.

3D Cell Culture Preparation. Cell suspensions were obtained by harvesting roughly 80% confluent adherent human fibroblasts using 0.05% trypsin-EDTA. Cells were centrifuged (2000 rcf, 5 min) and resuspended in a cell culture medium. The cell number was determined in a Neubauer hemacytometer using the trypan blue exclusion method, and the cell pellet containing the desired cell number was centrifuged (2000 rcf, 5 min) for the following embedding procedure.

Scaffolds for ^{1}H T_1-dependent oxygen quantification were realized as described previously.[5,18] Briefly, cell pellets were diluted in 500 μL of cell culture medium and 500 μL of liquid collagen-based membrane matrix, inserted in a sterile infusion

https://doi.org/10.1021/acs.analchem.3c02314
Anal. Chem. XXXX, XXX, XXX−XXX

tube (Volumed-Set Silicone), and subsequently polymerized at 310 K in a cell culture water bath. The polymerized cylindrical 3D gel containing the cells was softly aspirated in a new sterile infusion tube, connected to a 1 mL volume pipet to create the suction pressure, and gently released into the NMR bioreactor tube. In scaffolds prepared for comparison using ^{19}F T_1-dependent oxygen quantification, the medium was complemented with 250 μL perfluorotributylamine (PFTBA) doped microcarriers Cytodex 1 beads.

In both cases, after polymerization, the 3D scaffold was gently released into a Petri dish containing 35 mL medium and incubated for 24 h.[5,18]

Preparation for the NMR Measurement. The 3D scaffold was taken up from the Petri dish using an infusion tube and gently inserted into the InsightCell glass tube, clamped on the upper surface of a 1 cm-high bottom gel plug, as described elsewhere.[18] The glass tube was then connected to the bioreactor tube and placed within the NMR spectrometer.

NMR Bioreactor Setup. NMR experiments were performed on a 500.13 MHz Bruker Avance II spectrometer (Bruker BioSpin, Billerica, MA, USA). The instrument is equipped with a 5 mm ATM BBFO probe with a z-gradient used for high resolution liquid state NMR experiments. A cell culture bioreactor system within the NMR spectrometer was employed and previously established.[5] This setup was subsequently used for intra- and extracellular metabolic investigations of cell culture samples.[16] It makes use of a flow tube (InsightMR, Bruker) and its further specialization InsightCell, previously used in NMR studies of perfused cells.[16,17] The bioreactor was perfused using MEM supplemented with 1× nonessential amino acids (100 μM glycine, L-alanine, L-asparagine, L-aspartic acid, L-glutamic acid, L-proline, L-serine) (GIBCO/Invitrogen), 2 mM L-glutamine, 200 μM uridine, 1 mM sodium pyruvate, 100 U mL^{-1} penicillin, 100 μg/mL streptomycin, 10 μg/mL chlortetracycline, and 5% D2O in all experiments on cell culture samples. All experiments involving cells were carried out at 310 K and 5% CO2.

^{19}F NMR for Oxygen Quantification Using PFTBA Carriers. ^{19}F spin−lattice relaxation rate measurements were performed for oxygen quantification as described elsewhere.[5] The carrier frequency for the ^{19}F NMR measurement of PFTBA was set to the $\delta(-CF3)$ resonance at 83.3 ppm[5,27] in order to match the excitation bandwidth to the analyzed PFTBA $\delta(-CF_3)$ resonance.

All T_1 measurements were performed using a pseudo 2D inversion recovery 180°-τ-90° pulse sequence (*t1pir*) using 8 incremented delay times (between 0.005 and 6.3 s) with 4−8 scans per time increment (total measurement time of 5−10 min). 1D spectra were manually phased and baseline corrected. Bruker Topspin software (version 3.2, patch level 5) was used for calculating T_1 relaxation times based on $I[t_{IR}] = I[0] \times (1 - 2a \times \exp(-t_{IR}/T_1))$. All T_1 measurements were then converted into dissolved oxygen concentrations in reference to the previously established calibration curve.[5]

^1H NMR FOR OXYGEN QUANTIFICATION

Establishment of the $T_1^{-1}[s^{-1}]$–$O_2[\%]$ Calibration Curve. The relationship between T_1 relaxation times of the water resonance in dependence of the partial pressure of dissolved oxygen was determined on control medium measurements, saturated with 17 different atmospheric compositions (between 0% and 95% O_2.. Partial pressure of dissolved oxygen values between 21% and 95% were obtained saturating the solution for 5 min using a self-constructed gas blending system, previously established in our facility,[5] with always 5% CO_2. Values between 0% and 21% were obtained by bubbling the solution for 5 min with nitrogen (N_2), sonicating it for 1 min, and collecting samples at different time points until an equilibrium with atmospheric oxygen pressure. For each gas composition, the oxygen concentration was measured using an external oxygen sensor (Mettler-Toledo OptiOx) prior to insertion in the NMR tube. ^1H NMR measurements were then performed using a modified pseudo 2D inversion recovery 180°-τ_{IR}-90° pulse sequence (modified *t1pir*) using 16 incremented delay times (between 0.005 and 6 s) with 1 scan per time increment (measurement time ≈5 min) in the presence of a spoiler gradient ("sin.100" pulse, 70% intensity, 3 ms duration). 1D spectra were manually phased and baseline corrected, and T_1 relaxation times were determined as indicated above for ^{19}F.

All ^1H NMR T_1 measurements on water were converted to dissolved oxygen concentrations in reference to the calibration curve.

In situ Intracellular Oxygen Determination Using T_1 (^1H) Estimations Combined with Diffusion Measurements. ^1H NMR relaxation time measurements aiming at separating intra- and extracellular O_2 levels were performed using a pseudo-2D inversion recovery sequence combined with a diffusion filter, using a stimulated echo experiment with bipolar gradient pulses and a longitudinal eddy current delay (led)). The measurements were performed using 8 incremented delay times (between 0.05 and 6 s) with 4 acquisitions per time increment (≈ 5 min) in the presence of a spoiler gradient (sin.100 pulse, 70% intensity, 3 ms duration) after the inversion pulse, data size of 32 K, and acquisition time of 2.73 s. The selected diffusion time $\Delta$was 43 ms, and the gradient pulse length δ was 6 ms. 1D spectra were manually phased and baseline-corrected and relaxation times determined as noted above. Determination of T_1 times in relaxation measurements during flow periods accounted for inflowing unlabeled spins into the sensitive volume. This was accomplished by fitting T_1 according to

$$I[t_{IR}] = \frac{I_0}{V_{sens}} \times ((V_{sens} - t_{IR} \times \mathrm{flr}) \times (1 - 2a \times e^{-t_{IR}/T_1}) + t_{IR} \times \mathrm{flr}) \quad (1)$$

where V_{sens} is the NMR sensitive volume, I_0 is the magnetization at time point 0, t_{IR} is the inversion recovery time, and flr is the flow rate.

The analysis was performed by using MatLab software (R2020b, The Math-Works Inc., Natick, MA, USA).

Spatially Resolved Oxygen Determination Using T_1 (^1H) Estimations Combined with Pulsed Magnetic Field Gradients. For spatially resolved oxygen determination, ^1H NMR T_1 measurements were performed using a modified standard profile sequence (calibgp) with a preceding inversion recovery block. Sixteen incremented delay times (between 0.3 and 8 s) were applied with 1 scan per time increment (time of 7 min 30 s) in the presence of two spoiler compensation gradients (sin.20 pulse, 20% intensity, 3 ms duration) and a z gradient pulse (square pulse, 3% intensity, 6 ms duration) for spatial encoding. The z gradient was chosen such that the obtained water signal profile spread over large parts of the spectral bandwidth with sufficient resolution.

https://doi.org/10.1021/acs.analchem.3c02314
Anal. Chem. XXXX, XXX, XXX−XXX

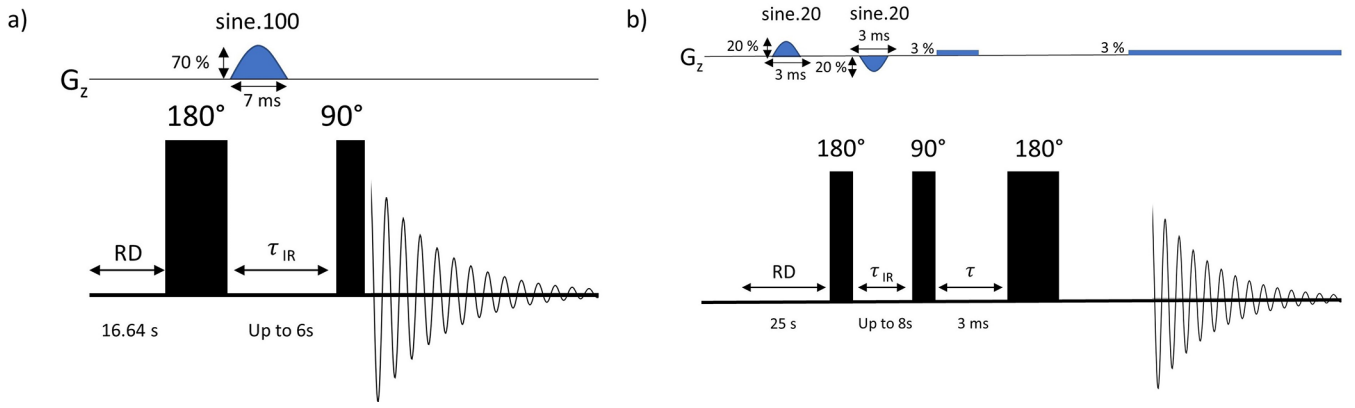

Figure 1. (a) Inversion recovery pulse sequence for global T_1 determination. (b) Modified inversion recovery pulse sequence for spatial encoding T_1 determination.

The spectral width was set to 100 kHz and digitized over 2048 data points. Signal acquisition time was 10.24 ms. 1D magnitude spectra were baseline corrected. Integration of the water profile was manually performed in Topspin software by cutting the profile peak into an arbitrary number of slices. T_1 relaxation times were calculated using Matlab program (R2020b, The Math-Works Inc., Natick, MA, USA) by fitting the curves of the integrated magnitude signal intensity according to $I[t_{IR}] = \text{abs}(I[0] \times (1-2a \times \exp(-t_{IR}/T_1)))$.

RESULTS AND DISCUSSION

We and others have previously demonstrated the capability to quantify oxygen content and oxygen consumption within 3D cell cultures, using relaxation time oxygen sensitivity of embedded fluorine atoms.[5] However, the deterioration of NMR signal quality caused by PFTBA beads in the 3D cell culture scaffold and a frequent insensitivity to oxygen changes rendered the prepared sample unusable,[18] prompting us to look for alternative solutions. In this study, we describe oxygen quantification approaches in living human 3D cell cultures in a perfused NMR bioreactor system: (I) T_1 estimation of water is implemented to determine the global concentration and consumption of oxygen throughout the NMR tube; solutions to suppress RD of very strong water resonance are discussed; (II) *in situ* intracellular oxygen content estimation using T_1 of slowly diffusing water molecules is implemented to determine local oxygen tension and consumption within 3D cell culture samples; and (III) spatially resolved oxygen levels along the tube using T_1 estimations of water profiles are determined to detect oxygen potential changes along the scaffold length.

Global Oxygen Determination Using T_1 (^{1}H) Estimations. In a first attempt to assess cellular oxygen without employing ^{19}F T_1 measurements, metabolites from a cell culture medium were tested for oxygen concentration-dependent T_1 relaxation times. Standard cell culture medium samples were therefore saturated with different oxygen concentrations, and inversion recovery T_1 estimations of metabolites were performed at 310 K. Nonoverlapping metabolite contributions were chosen for the analysis in order to avoid misinterpretation. Eight metabolites (glutamine, histidine, isoleucine, phenylalanine, pyruvate, tyrosine, uridine, and valine) and the internal standard trimethylsilyl propanoic acid (TSP) provided the largest T_1 relaxation time variation ranges at different oxygen saturation levels (Figure S1). However, relatively high variability and only moderate reproducibility between independent T_1 relaxation time of metabolite experiments were encountered. Furthermore, spectral analysis turned out to be very time-consuming which makes this approach rather impractical, especially in longitudinal studies. However, it might be possible to use this approach in cell lines with intracellular metabolites (e.g., NAA in brain cell cultures), because it directly yields intracellular oxygen tension.

The decrease of spin−lattice and spin−spin relaxation times, T_1 and T_2, respectively, upon the addition of paramagnetic ions to water has been known since the early days of NMR.[28] An inverse relationship between the T_1 relaxation of water and oxygen concentration was observed (Mihrej, 1965). We therefore investigated the dependency of T_1 relaxation times of water on oxygen tension, neglecting the contribution of low-concentration reactive oxygen species (ROS) produced by cellular oxidative phosphorylation. Standard cell culture medium samples were saturated with different oxygen concentrations, and inversion recovery T_1 estimations of water were performed at 310 K. The well-known radiation damping effects (see e.g., Keeler et al. or Mao et al.[22,29]) resulting in nonexponential signal behavior of the relaxation curves and very short relaxation times (see Figure S2) was tackled first by detuning the coil to reduce the quality factor,[23] which however did not provide a reliable solution. Second, pulsed field gradients ("spoiling gradient") were applied to dephase the transverse components of the magnetization.[30,31] In our study, the insertion of a spoiled gradient at the beginning of the recovery period along with an accurate optimization of both the inversion and readout pulse length solved the RD problem (Figure 1a) and allowed for stable and consistent quantitative T_1 relaxation time estimations of water.

Validation experiments were conducted in order to determine the feasibility and sensitivity of the T_1 relaxation time measurement to detect changes in the oxygen tension of cell culture systems under perfusion conditions. Measurements were performed with periodical flow-rate interruptions ("stop and go") of pure medium, saturated with 47% oxygen, accompanied by continuous T_1 measurements to evaluate possible influences of the flow on the estimated T_1 relaxation time of water. Considering the impact of inflowing spins into the sensitive region of the NMR volume during the T_1 estimation experiment (see eq 1) resulted in similar values with and without flow at low flow rates (0.1 mL/min). At higher flows (0.2 and 0.3 mL/min), increased variability of estimated T_1 was obtained, most likely due to turbulences.

https://doi.org/10.1021/acs.analchem.3c02314
Anal. Chem. XXXX, XXX, XXX−XXX

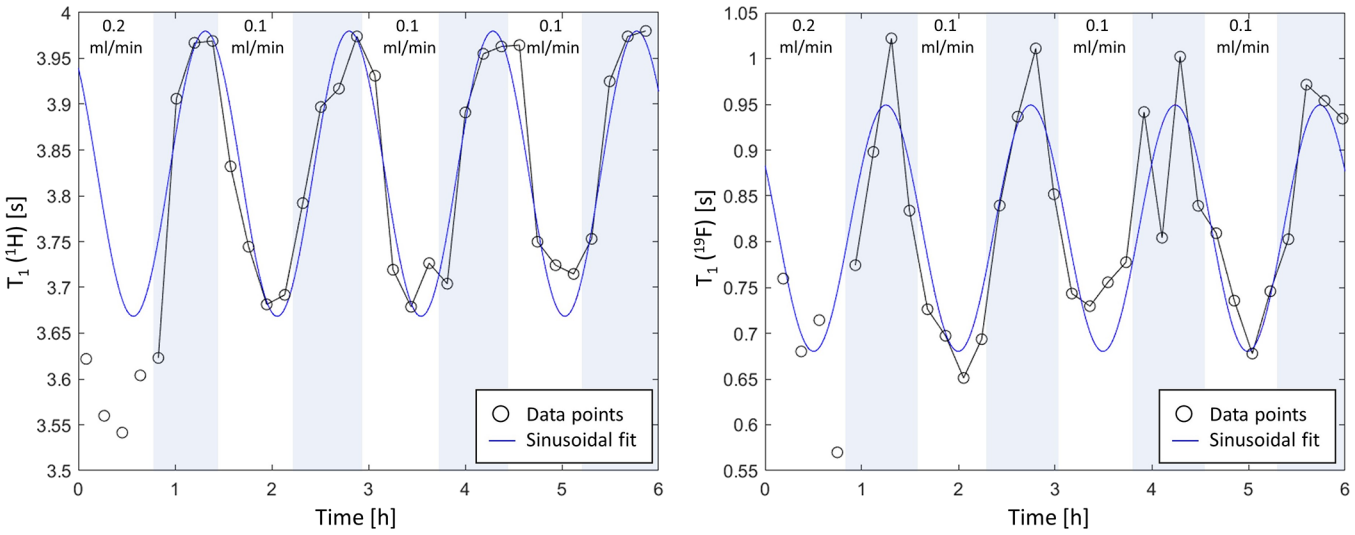

Figure 2. Plot of estimated ^{1}H (left) and ^{19}F (right) T_1 versus time in 3D collagen-based matrix embedded 10 million fibroblasts during interleaved stop (highlighted in blue) and go (at 0.1 mL min^{-1}) of the perfusion of medium containing 47% oxygen concentration. The blue line indicates fitting of the T_1 time curve to a sinusoidal function (leaving the initial period with higher flow).

Consequently, only low flow rates (0.1 mL/min) were used in subsequent measurements.

A measurement with periodical flow-rate interruptions ("stop and go") of the perfusion was performed in an experiment on 3D collagen-based matrix embedded fibroblasts and PFTBA coated beads and accompanied by interleaved ^{1}H and ^{19}F T_1 measurements. The rationale was a comparison of ^{1}H T_1 adaptations upon challenges with the previously determined ^{19}F T_1 changes.[5] Interruption of the perfusion rate for ~40 min resulted in an increase of both ^{1}H and ^{19}F T_1 relaxation times, corresponding to a decrease of the oxygen tension in the bioreactor tube due to ongoing cellular respiration (Figure 2). Moreover, measured ^{1}H and ^{19}F T_1 values showed a correlation factor of 0.65 ($p < 0.001$). In fact, in this specific measurement, the ^{1}H determined T_1 time curve appears smoother and to better follow the periodic flow change than those determined via ^{19}F measurements. This was also shown by a lower fitting deviation of the ^{1}H determined T_1 time curve to an assumed sinusoidal function, compared to the ^{19}F determined T_1 time curve (RMSE(^{1}H) = 0.047; RMSE-(^{19}F) = 0.055). Therefore, the feasibility and sensitivity of the ^{1}H T_1 relaxation time measurement to detect changes in oxygen tension in the bioreactor tube were demonstrated.

Based on these results, calibration measurements were performed of water T_1 relaxation times in dependence of the partial pressure of dissolved oxygen at an operating temperature of 310 K. The calibration curve is shown in Figure 3. As expected, a linear relationship between the relaxation rate ($1/T_1$) and the partial pressure oxygen (pO_2) was obtained.

***In Situ* Intracellular Oxygen Determination Using Slow Diffusing T_1 (^{1}H) Estimations.** In our previous study we found that only 1−2% of total water in the sample volume within the sensitive NMR region was compartmentalized within cell membranes of the investigated fibroblasts,[18] which is in agreement with previous studies (Pilatus et al., 1997, Van Zijl et al., 1991). Therefore, the oxygen content determined with the global T_1 relaxation time technique mainly reflects the oxygen level in the extracellular space, potentially obscuring the interpretation of possible oxygen changes in the vicinity of the cells. During prolonged stop of the perfusion periods (in

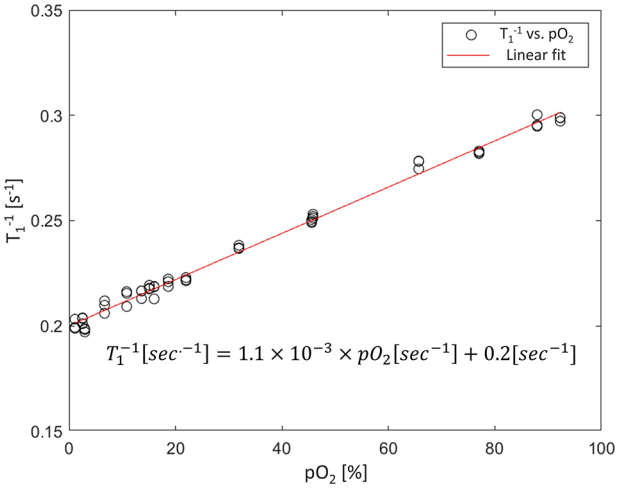

Figure 3. T_1 relaxation time of the water resonance in dependence of the partial pressure of dissolved oxygen (pO_2) at an operating temperature of 310 K.

"stop and go" experiments), global oxygen content never reached levels close to zero as we expected due to cellular respiration, and local hypoxia regions could not be detected with the global oxygen estimation. However, we have previously shown the capability to separately measure the intracellular and extracellular water contribution using diffusion NMR. The combination of proton spin−lattice relaxation time T_1 and diffusion measurements of water at high diffusion-weighting factor might, therefore, also allow for determining intracellular or *in situ* oxygen content. "Stop and go" (periodical flow-rate interruptions) of the perfusion was performed in an experiment on 3D collagen-based matrix embedded fibroblasts and overall and *in situ* directly at the cells T_1 measurements of water were continuously conducted (Figure 4). *In situ* and intracellular estimated T_1 values were found to be lower compared to overall T_1 values (3.6−4 and 4.3−4.5 s, respectively), in agreement with,[32,33] where a faster spin−lattice relaxation of intracellular water was found. However, estimated T_1s of compartmentalized water in 3D

https://doi.org/10.1021/acs.analchem.3c02314
Anal. Chem. XXXX, XXX, XXX−XXX

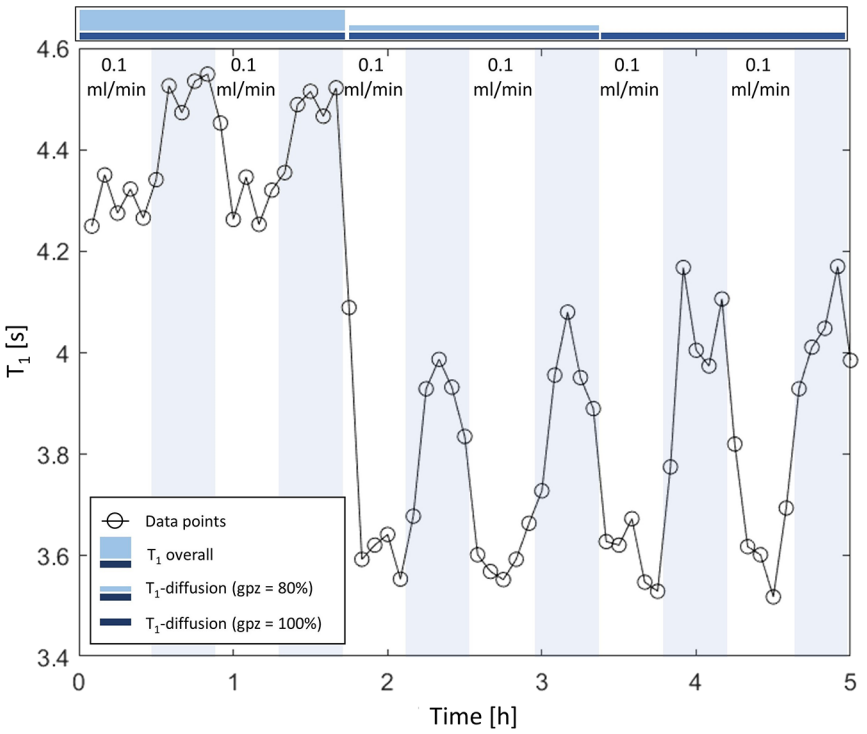

Figure 4. Plot of estimated overall and *in situ* (gpz = 80%, 100%) T_1 versus time in 3D collagen-based matrix embedded 10 million fibroblasts during interleaved *stop* (highlighted in blue) and *go* (at 0.1 mL min^{-1}) of the perfusion of medium containing 21% oxygen concentration.

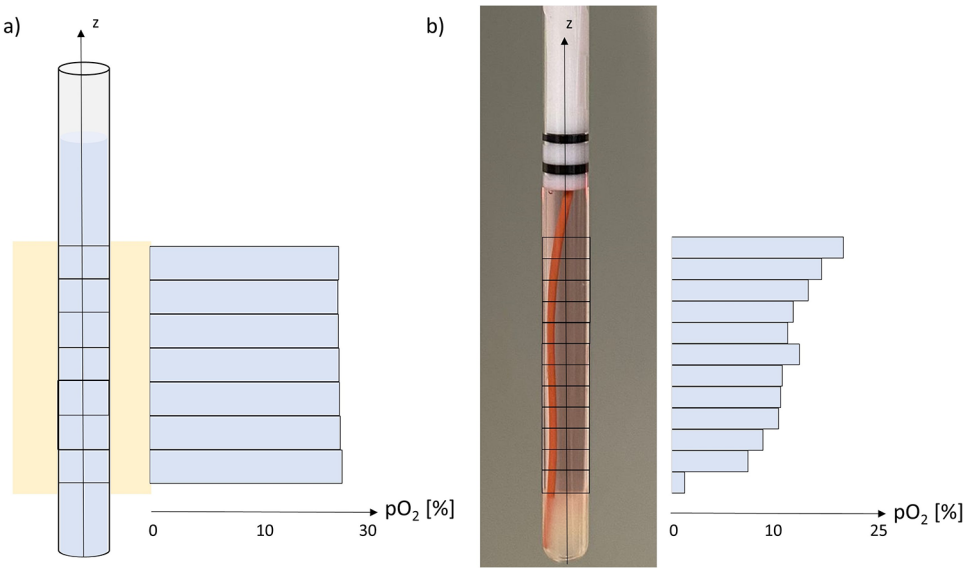

Figure 5. (a) Spatially resolved T_1 relaxation time estimation of a homogeneous H_2O sample at an operating temperature of 310 K. Seven profile sections were selected for the analysis. (b) Spatially resolved T_1 relaxation time estimation of a cell pellet placed at the bottom of the bioreactor tube was performed at an operating temperature of 310 K. Twelve profile sections were selected for the analysis.

embedded fibroblasts were longer than values measured in pelleted fibroblasts (≈ 2.5 s) at 37 °C, in agreement with T_1s found in literature,[34,35] likely due to T_1 estimation of either water molecules attached to membranes or of a mixture of intra- and extracellular contributions.[36−38] However, T_1 differences between "stop" and "go" periods of the perfusion were higher *in situ* and intracellularly than in the extracellular space, thus facilitating the detection of small cellular oxygen changes. In an attempt to establish a calibration curve for intracellular oxygen, medium saturated with 4 different atmospheric compositions was used in an experiment on continuously perfused 3D collagen-based matrix embedded fibroblasts and interleaved overall, and *in situ* directly at the cells T_1 measurements of water were conducted. This calibration would rely on only negligible cellular oxygen consumption and metabolic status changes. However, high variability of estimated *in situ* and intracellular T_1 values at different dissolved oxygen concentration (up to 22%) was encountered; therefore, the establishment of an intracellular T_1-O_2 calibration curve appeared unfeasible. Interleaved ATP measurements indicated the high viability of the cells at the different oxygen levels. T_1 changes due to cell death can

https://doi.org/10.1021/acs.analchem.3c02314
Anal. Chem. XXXX, XXX, XXX−XXX

therefore not explain the variances. These might be explained by the increasing contribution of reactive oxygen species (ROS) in the intracellular space[39] and the low cellular fraction within the sensitive NMR volume. Further improvements will be needed to minimize the variability of estimated T_1s, for example, by increasing the intra- to extracellular volume ratio in cell types other than fibroblasts. Still, it appears feasible to determine relative T_1 changes indicating intracellular oxygen changes in longitudinal investigations, but without quantitative determination.

Spatially Resolved Oxygen Determination Using T_1 (^{1}H) Estimations Combined with Pulsed Magnetic Field Gradients. While the combination of proton spin−lattice relaxation time T_1 and diffusion measurements of water at high diffusion-weighting factor b allows to monitor oxygen levels *in situ* at the cells, a spatially resolved oxygen determination would be extremely useful to investigate the heterogeneity of oxygen concentration, to detect local hypoxia regions, and to study oxygen diffusion within the 3D scaffold volume. ^{19}F NMR coupled with PFC-containing particles has been used to noninvasively investigate the spatiotemporal evolution of oxygen distribution in microbial impacted packed bed systems.[15] Using this approach, spatial oxygen gradients and the comprehensive interplay between fluid dynamics and oxygen transport phenomena were studied. However, to our knowledge no study has focused on the spatially resolved oxygen tension using T_1 relaxation time estimations of water. In this study, a modified inversion recovery pulse sequence with a readout magnetic field gradient for spatial encoding was employed (Figure 1b). Compensation of the spoiler gradients removed eddy currents, causing wiggles in the oxygen profile. Two validation experiments were conducted to determine the sensitivity of the spatially resolved oxygen determination method. In the first test, spatially resolved T_1 estimation of a homogeneous water sample at 310 K was performed. The ^{1}H spectral profile was split into 7 sections and T_1 determined. Very similar T_1 values were obtained for all seven sections (T_1 = 4.37 ± 0.004 s), corresponding to a very stable spatially distributed oxygen content of ∼25% along the bioreactor tube (Figure 5a). In a second experiment, spatially resolved T_1 relaxation time estimation of a cell pellet placed at the bottom of the bioreactor tube was performed at 310 K. Analysis of 12 profile sections led to T_1 values ranging from 4.71 s (at the bottom, close to the cell pellet) to 4.40 s (at the top, distant from the cells), corresponding to oxygen values between 0% (due to ongoing cellular respiration) and 25% (value close to the oxygen saturation level found in the homogeneous water sample), respectively (Figure 5b). The experiments demonstrate that the method provides sufficient sensitivity that is necessary to detect spatially resolved oxygen tension along the bioreactor tube.

The strength of the presented approach for real-time monitoring of spatially resolved oxygen tension lies in the possibility to detect potential (temporal) oxygen gradients between the perfusion inlet and outlet within the tube, to detect possible local hypoxic regions inside the scaffold, or to characterize scaffold and cellular distribution homogeneity.

CONCLUSIONS

The methods described in this paper to longitudinally monitor global, *in situ* intracellular, and spatially resolved oxygen tension in 3D cell cultures are of potential value for investigating oxygen consumption as surrogate marker of OXPHOS, without the need to use external sensors (i.e., PFCs) that first can interfere with the quality of NMR measurements, second quite often fail to yield the required rapidly adjusting oxygen sensitivity, and third greatly ease the sample preparation of 3D matrix embedded cells. The inclusion of the presented oxygen quantification techniques in a study protocol provides the possibility to measure mitochondrial respiration and metabolic changes simultaneously. For in situ measurements, it should be noted, however, that the indirectly determined absolute oxygen values based on relaxation time measurements are not reliable due to the concurrent presence of ROS and paramagnetic metal ions also affecting T_1. Nevertheless, in longitudinal measurements, relaxation time changes probably indicate relative oxygen changes. The low cellular volume of fibroblasts possibly adds to the variability of the in situ T_1 estimations. It is likely that higher cellular volume, i.e., increased intra- to extracellular volume ratio in cell types other than fibroblasts lowers the variability.

Furthermore, the inclusion of oxygen measurements by using spin−spin (T_2) relaxation time estimations is anticipated for futures studies.

ASSOCIATED CONTENT

Supporting Information

The Supporting Information is available free of charge at https://pubs.acs.org/doi/10.1021/acs.analchem.3c02314.

TAdditional figures (S1−S3) as mentioned in the text of: the calibration of T_1 relaxation times of metabolites and partial pressure of dissolved oxygen (pO_2), the radiation damping effect on the relaxation curve of water, and the estimated ^{1}H flow-corrected and non flow-corrected T_1 versus time in culture medium (PDF)

AUTHOR INFORMATION

Corresponding Author

Peter Vermathen − *Translational Imaging Center (TIC), Swiss Institute for Translational and Entrepreneurial Medicine, 3010 Bern, Switzerland; Departments of Biomedical Research and Neuroradiology, University of Bern, 3012 Bern, Switzerland*; Email: peter.vermathen@dbmr.unibe.ch

Authors

Christian Urzì − *Departments of Biomedical Research and Neuroradiology, University of Bern, 3012 Bern, Switzerland; Department of Clinical Chemistry, University Hospital Bern, 3010 Bern, Switzerland; Graduate School for Cellular and Biomedical Sciences, University of Bern, 3012 Bern, Switzerland*; orcid.org/0000-0002-3048-9877

Christoph Meyer − *Departments of Biomedical Research and Neuroradiology, University of Bern, 3012 Bern, Switzerland; Department of Clinical Chemistry, University Hospital Bern, 3010 Bern, Switzerland; Graduate School for Cellular and Biomedical Sciences, University of Bern, 3012 Bern, Switzerland*

Jean-Marc Nuoffer − *Department of Clinical Chemistry, University Hospital Bern, 3010 Bern, Switzerland; Department of Pediatric Endocrinology, Diabetology and Metabolism, University Children's Hospital of Bern, 3010 Bern, Switzerland*

Complete contact information is available at:

https://doi.org/10.1021/acs.analchem.3c02314
Anal. Chem. XXXX, XXX, XXX−XXX

https://pubs.acs.org/10.1021/acs.analchem.3c02314

Author Contributions

#J.-M.N. and P.V. contributed equally to this work.

Author Contributions

C.U. designed and conducted the experiments, administrated the project, collected and analyzed the data, wrote, reviewed, and edited the manuscript. C.M. reviewed and edited the manuscript. J.M.N. provided resources and funding, supervised the project, and reviewed and edited the manuscript. P.V. provided resources and funding, supervised the project, and reviewed and edited the manuscript. The manuscript was written through contributions of all authors. All authors have given approval to the final version of the manuscript.

Notes

The authors declare no competing financial interest.

■ ACKNOWLEDGMENTS

We would like to thank the Swiss National Science Foundation SNF (Nr. 310030_192691), who funded the project. We would like to thank also the Batzebär foundation of the children's university hospitals Bern, who also supported financially the project.

■ REFERENCES

(1) Graeber, T. G.; Peterson, J. F.; Tsai, M.; Monica, K.; Fornace, A. J.; Giaccia, A. *Mol. Cell. Biol.* **1994**, *14*, 6264−6277.
(2) Mercille, S.; Massie, B. *Cytotechnology.* **1994**, *15*, 117−128.
(3) Erecinska, M.; Silver, I. A. *Respiration Physiology* **2001**, *128*, 263−276.
(4) Oomen, P. E.; Skolimowski, M. D.; Verpoorte, E. *Lab Chip* **2016**, *16*, 3394−3414.
(5) Hertig, D.; Maddah, S.; Memedovski, R.; Kurth, S.; Moreno, A.; Pennestri, M.; Felser, A.; Nuoffer, J. M.; Vermathen, P. *Analyst* **2021**, *146*, 4326−4339.
(6) Kieninger, J.; Tamari, Y.; Enderle, B.; Jobst, G.; Sandvik, J. A.; Petterson, E. O.; Urban, G. A. *Biosensors* **2018**, *8*, 44.
(7) Fang, Y. *ASSAY and Drug Development Technology* **2006**, *4*, 5.
(8) Gruber, P.; Marques, M. P C.; Szita, N.; Mayr, T. *Lab Chip* **2017**, *17*, 2693−2712.
(9) Zdrazilova, L.; Hansikova, H.; Gnaiger, E. *PLoS One* **2022**, 17.
(10) Makrecka-Kuka, M.; Krumschnabel, G.; Gnaiger, E. *Biomolecules* **2015**, *5*, 1319−1338.
(11) Ferrick, D. A.; Neilson, A.; Beeson, C. *Drug Discovery Today* **2008**, *13*, 268−274.
(12) Hertig, D.; Felser, A.; Diserens, G.; Kurth, S.; Vermathen, P.; Nuoffer, J. M. *Metabolomics* **2019**, 15−32.
(13) Ruiz-Cabello, J.; Walczak, P.; Kedziorek, D. A.; Chacko, V. P.; Schmieder, A. H.; Wickline, S. A.; Lanza, G. M.; Bulte, J. W. M. *Magn. Reson. Med.* **2008**, *60*, 1506−1511.
(14) Pilatus, U.; Aboagye, E.; Artemov, D.; Mori, N.; Ackerstaff, E.; Bhujwalla, Z. M. *Magn. Reson. Med.* **2001**, *45*, 749−755.
(15) Simkins, J. W.; Stewart, P. S.; Seymour, J. D. *J. Magn. Reson.* **2018**, *293*, 123−133.
(16) Cerofolini, L.; Giuntini, S.; Barbieri, L.; Pennestri, M.; Codina, A.; Fragai, M.; Banci, L.; Luchinat, E.; Ravera, E. *Biophys. J.* **2019**, *116* (2), 239−247.
(17) Luchinat, E.; Barbieri, L.; Campbell, T. F.; Banci, L. *Anal. Chem.* **2020**, *92*, 9997−10006.
(18) Urzì, C.; Hertig, D.; Meyer, C.; Maddah, S.; Nuoffer, J. M.; Vermathen, P. *International Journal of Molecular Sciences* **2022**, *23*, 6555.
(19) Lee, A. L.; Gee, C. T.; Weegman, B. P.; Einstein, S. A.; Juelfs, A. R.; Ring, H. L.; Hurley, K. R.; Egger, S. M.; Swindlehurst, G.; Garwood, M.; Pomerantz, W. C.; Haynes, C. L. *ACS Nano* **2017**, *11*, 5623−5632.
(20) Interstate Technology & Regulatory Council. Technical Resources for Addressing Environmental Releases of Per- and Polyfluoroalkyl Substances (PFAS). https://pfas-1.itrcweb.org/ (accessed 2023−05−16).
(21) Mihrej, M. E. *Can. J. Chem.* **1965**, 43.
(22) Keeler, A.; Whitney, H. M. *Spectrosc. Lett.* **2015**, *48* (10), 781−786.
(23) Eykyn, T. R.; Payne, G. S.; Leach, M. O. *Phys. Med. Biol.* **2005**, *50*, N371−N376.
(24) Pilatus, U.; Shim, H.; Artemov, D.; Davis, D.; Van Zijl, P. C. M.; Glickson, J. D. *Magn. Reson. Med.* **1997**, *37*, 825−832.
(25) Van Zijl, P. C. M.; Moonen, C. T. W.; Faustino, P.; Pekar, J.; Kaplan, O.; Cohen, J. S. *Proc. Natl. Acad. Sci. U. S. A.* **1991**, *88*, 3228−3232.
(26) Bottomley, P. A. *Ann. N.Y. Acad. Sci.* **1987**, *508*, 333−48.
(27) Ribeiro, A. A.; Umayahara, K. *Magn. Reson. Chem.* **2003**, *41*, 107−114.
(28) Bloembergen, N.; Purcell, E. M.; Pound, R. V. *Physical Review Journals Archive* **1948**, *73*, 7.
(29) Mao, X.-A.; Wu, D. H.; Ye, C. H. *Chem. Phys. Lett.* **1993**, 204.
(30) Zhou, J.; Mori, S.; Van Zijl, P. C. M. *Magn. Reson. Med.* **1998**, *40* (5), 712−719.
(31) Lu, H.; Clingman, C.; Golay, X.; Van Zijl, P. C. M. *Magn. Reson. Med.* **2004**, *52*, 679−682.
(32) Mauss, Y.; Grucker, D.; Fornasiero, D.; Chambron, J. *Magn. Reson. Med.* **1985**, *2*, 187−194.
(33) Humpfer, E.; Spraul, M.; Nicholls, A. W.; Nicholson, J. K.; Lindon, J. C. *Magn. Reson. Med.* **1997**, *38*, 334−336.
(34) Callahan, D. E.; Deamond, S. F.; Creasey, D. C.; Trapane, T. L.; Bruce, S. A.; Ts'o, P. O. P.; Kan, L. S. *Magn. Reson. Med.* **1991**, *22* (1), 68−80.
(35) Callahan, D. E.; Trapane, T. L.; Deamond, S. F.; Kao, G.; Ts'o, P. O. P.; Kan, L. S. *Magn. Reson. Med.* **1991**, *18* (3), 193−202.
(36) Eriksson, S.; Elbing, K.; Söderman, O.; Lindkvist-Petersson, K.; Topgaard, D.; Lasic, S. *PLoS One* **2017**, *12*, 5.
(37) Haida, M.; Yamamoto, M.; Matsumura, H.; Shinohara, Y.; Fukuzaki, M. *Journal of Cerebral Blood Flow and Metabolism* **1987**, *7*, 552−556.
(38) Quirk, J. D.; Bretthorst, G. L.; Duong, T. Q.; Snyder, A. Z.; Springer, C. S.; Ackerman, J. J. H.; Neil, J. J. *Magn. Reson. Med.* **2003**, *50*, 493−499.
(39) Hollen, C.; Neilson, L. E.; Barajas, R. F., Jr.; Greenhouse, I.; Spain, R. I. *Frontiers in Neurology* **2023**, 13.